RSC Advances

PAPER

View Article Online
View Journal | View Issue

Cite this: *RSC Adv.*, 2023, **13**, 30978

Synthesis of optically active star polymers consisting of helical poly(phenylacetylene) chains by the living polymerization of phenylacetylenes and their chiroptical properties†

Ayato Inaba,[a] Tatsuya Nishimura, *[a] Masato Yamamoto,[a] Sandip Das,[b] Ayhan Yurtsever,[b] Kazuki Miyata,[b] Takeshi Fukuma,[b] Seigo Kawaguchi,[c] Moriya Kikuchi,[d] Tsuyoshi Taniguchi[b] and Katsuhiro Maeda *[ab]

Received 1st September 2023
Accepted 17th October 2023

DOI: 10.1039/d3ra05971e

rsc.li/rsc-advances

Star polymers consisting of three helical poly(phenylacetylene) chains with a precisely controlled molecular weight (molar mass dispersity < 1.03) were successfully synthesized by the living polymerization of phenylacetylene derivatives with a Rh-based multicomponent catalyst system comprising trifunctional initiators, which have three phenylboronates centered on a benzene ring, the Rh complex $[Rh(nbd)Cl]_2$, diphenylacetylene, triphenylphosphine, and a base. The analysis of chiroptical properties of the optically active star polymers obtained by the living polymerization of optically active phenylacetylene derivatives revealed that the star polymers exhibited chiral amplification properties owing to their unique topology compared with the corresponding linear polymers.

Introduction

Star polymers are typical topological polymers that have attracted significant attention owing to their unique structures and physical properties.[1,2] Star polymers possess a spherical shape and a space in their inner parts, allowing them to be applied as, for example, drug delivery materials.[3,4] Furthermore, star polymers become potential candidates for biocompatible materials when sugar residues are introduced at the ends of the arms.[5,6] Thus, star polymers are expected to be new materials that play important roles in the field of nanotechnology.[7,8] Three main approaches are widely used for the synthesis of star polymers: (1) living polymerization using multifunctional initiators with multiple initiating points (graft-from method), (2) coupling reaction between multifunctional coupling agents and linear living polymers (graft-to method, core-first method), and (3) reaction between living chain ends and a small number of bifunctional monomers (arm-first method).[2] Precise polymerization control is essential for the synthesis of star polymers with the desired structures. The development of various living polymerization techniques, such as ATRP[9,10] and RAFT,[11] has facilitated the synthesis of star polymers consisting of vinyl, conjugated, or helical polymers, with numerous successful examples reported.[12–19] In particular, chiral helical star polymers exhibit optical properties that distinguish them from conventional non-helical star polymers. These unique properties make them promising candidates for a wide range of applications in chiral materials, such as chiral stationary phases and asymmetric catalytic scaffolds.

Recently, we have developed a new living polymerization technique for phenylacetylene derivatives using a Rh-based multicomponent catalyst system consisting of a commercially available rhodium complex, a phenylboronic acid derivative, diphenylacetylene (DPA), triphenylphosphine (PPh_3), and a base.[20–22] This polymerization technique enables not only the synthesis of *cis*-stereoregular poly(phenylacetylene) with a precisely controlled molecular weight and narrow molecular weight dispersion but also facilitates the introduction of desired functional groups at the ends of the polymer chain.[23]

In this study, we report the synthesis of star polymers consisting of three poly(phenylacetylene) chains with precisely controlled chain lengths through the living polymerization of phenylacetylene derivatives using our Rh-based multicomponent catalyst system.[24] We also explored the relationship between the structures and functions of these star polymers. The obtained star polymers were thoroughly characterized using various spectroscopic techniques, and atomic force

[a]*Graduate School of Natural Science and Technology, Kanazawa University, Kakuma-machi, Kanazawa 920-1192, Japan. E-mail: nishimura@se.kanazawa-u.ac.jp; maeda@se.kanazawa-u.ac.jp*

[b]*Nano Life Science Institute (WPI-NanoLSI), Kanazawa University, Kakuma-machi, Kanazawa 920-1192, Japan*

[c]*Department of Organic Materials Science, Graduate School of Organic Materials Science, Yamagata University, 4-3-16, Jonan, Yonezawa 992-8510, Japan*

[d]*Faculty of Engineering, Yamagata University, 4-3-16, Jonan, Yonezawa 992-8510, Japan*

† Electronic supplementary information (ESI) available. See DOI: https://doi.org/10.1039/d3ra05971e

microscopy (AFM) was employed to visualize their star-shaped structures clearly. Furthermore, we systematically investigated the differences in the chiroptical properties between the star polymers bearing three optically active helical poly(phenylacetylene) arms and the corresponding linear helical poly(phenylacetylene) chains of the same length as the arms of the star polymers to reveal the effect of polymer topology on the chiroptical properties of helical poly(phenylacetylene) chains.[25–27]

Results and discussion

The trifunctional boronic acid ester **A** was prepared according to previous reports (Scheme S1†).[28] A three-armed star-shaped poly(phenylacetylene) (**A**(poly-**1**$_n$)$_3$) with a precisely controlled molecular weight was synthesized using a living polymerization method with our Rh-based multicomponent catalyst system using **A** as the initiator (Scheme 1 and Table 1). An excess amount of [Rh(nbd)Cl]$_2$ ([Rh]/([**A**]/3) ≥ 1.5, nbd = norbornadiene) was used relative to the phenylboronate groups to ensure that the reaction between all of the boronate groups of the initiator **A** and the Rh complex proceeded completely. Initially, the catalyst solution was prepared by adding 50% (w/v) aqueous KOH to a THF solution of initiator **A**, [Rh(nbd)Cl]$_2$, and DPA, followed by stirring at 30 °C for 5 min. Then, PPh_3 was added to the solution to afford the catalyst solution. After the catalyst solution was diluted with THF, phenylacetylene (**1**) ([**1**]/([**A**]/3) = 50) was added to initiate the polymerization, and the polymerization reaction was carried out at 30 °C (run 1). After 1 h, acetic acid was added to terminate the polymerization reaction, and the product was precipitated in methanol to afford a yellow polymer in moderate yield.

The size-exclusion chromatography (SEC) measurement of the obtained polymer (run 1) showed apparent three peaks when three SEC columns connected in series were used (Fig. 1a). The number-average molar mass (M_n) of each peak was larger than that (15 000) calculated from the feed ratio ([**1**]/([**A**]/3) = 50). These results suggest that the initiation of the polymerization reaction was not strictly controlled under these conditions (run 1), and star polymers with different numbers of arms (one, two, or three) were formed from initiator **A**.

Table 1 Results of the polymerization of phenylacetylene (**1**) with a Rh-based multicomponent catalyst system using initiator **A**[a]

Run	Base	[Rh]/([**A**]/3)	Polymer		
			Yield[b] (%)	$M_n \times 10^{-4}$[c]	M_w/M_n[c]
1	50% KOH	1.5	65	—	—
2	10% KOH	1.5	85	1.4	1.03
3	10% KOH	2.0	92	1.3	1.05

[a] Reaction conditions: **A** (0.10 mmol), [Rh(nbd)Cl]$_2$ (0.05 mmol (runs 1 and 2), 0.067 mmol (run 3)), DPA (0.15 mmol (runs 1 and 2), 0.2 mmol (run 3)), in THF (0.2 mL) at 30 °C (run 1) or 0 °C (runs 2 and 3) for 10 min, then phenylacetylene (**1**) (1.7 mmol) and PPh_3 (0.15 mmol (runs 1 and 2), 0.2 mmol (run 3)) in THF (3.8 mL) at 30 °C for 1 h. [b] Methanol-insoluble part. [c] Determined by SEC using three columns (TSKgel G4000H$_{XL}$ + G3000H$_{XL}$ + G3000H$_{XL}$) connected in series based on polystyrene standards (THF, 40 °C).

In this multicomponent catalytic system, the hydrolysis of phenylboronate groups during catalyst preparation is important for the initiation of polymerization.[20] Therefore, we used 10% (w/v) aqueous KOH as the base to promote the hydrolysis of phenylboronate (pinacolborate) groups by increasing the amount of water (runs 2 and 3). SEC measurements of the resulting polymers showed nearly a single peak derived from the three-armed star polymer (Fig. 1b and c). When the amount of the Rh complex used was increased, the yield of the polymer increased (run 3), and the molecular weight of the obtained polymer (M_n = 13 000) was almost the same as that calculated from the feed ratio (run 3). In the SEC chromatogram of run 3 (Fig. 1c), a subtle shoulder assignable to a two-armed polymer was observed, while no peak due to a one-armed polymer was observed. The generation of the two-armed polymer could be attributed to steric hindrance arising from the introduction of two rhodium complexes into the core, which could affect the efficiency of the introduction of the third rhodium complex.

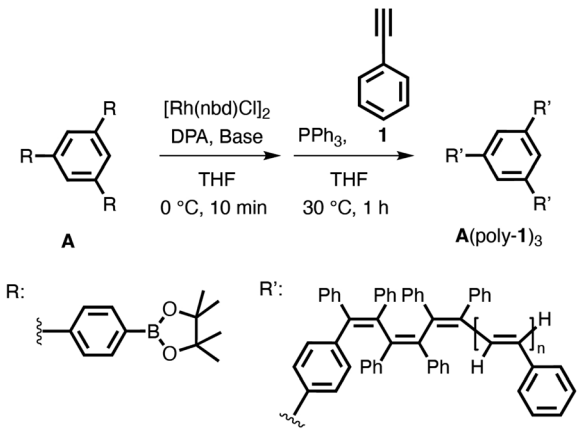

Scheme 1 Synthesis of a three-armed star-shaped poly(phenylacetylene) derivative (**A**(poly-**1**)$_3$) with a Rh-based multicomponent catalyst system using trifunctional phenylboronate **A** as the initiator.

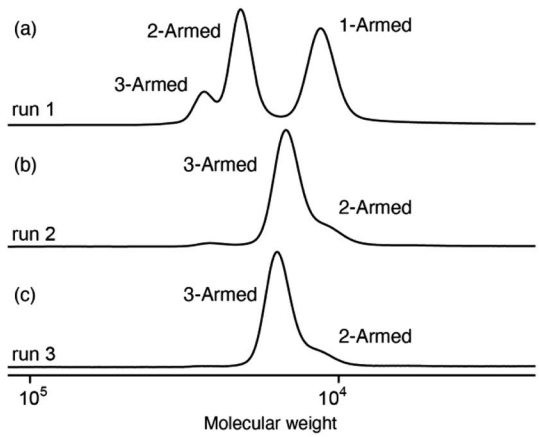

Fig. 1 SEC chromatograms of the obtained **A**(poly-**1**)$_3$ ((a) run 1, (b) run 2, and (c) run 3 in Table 1).

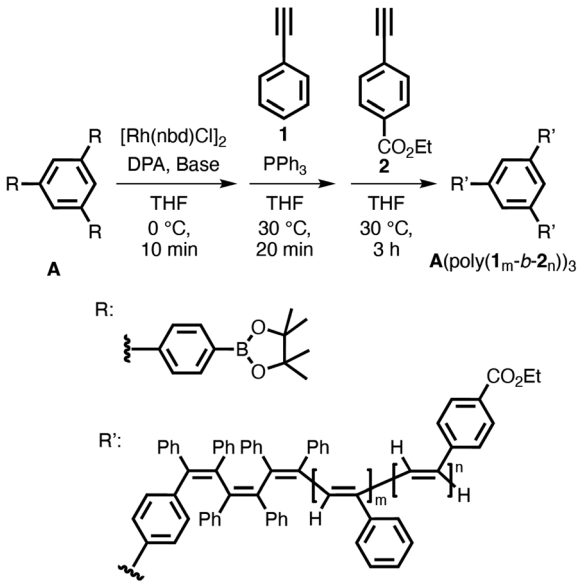

Scheme 2 Synthesis of star-shaped block copolymer A(poly($\mathbf{1}_m$-*b*-$\mathbf{2}_n$))$_3$ composed of different phenylacetylene derivatives (**1** and **2**) using initiator **A**.

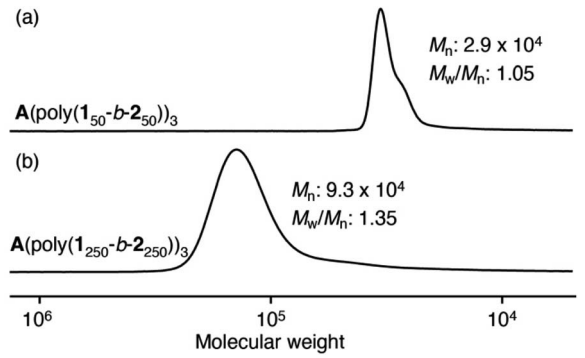

Fig. 2 SEC chromatograms of block-type star polymers A(poly($\mathbf{1}_m$-*b*-$\mathbf{2}_n$))$_3$ in multistage copolymerization of phenylacetylenes (1st stage: **1**, 2nd stage: **2**) with a Rh-based multicomponent catalyst system using initiator **A** ((a) A(poly($\mathbf{1}_{50}$-*b*-$\mathbf{2}_{50}$))$_3$ and (b) A(poly($\mathbf{1}_{250}$-*b*-$\mathbf{2}_{250}$))$_3$).

Based on these results, it was considered that the polymerization proceeded uniformly from all three starting points of initiator **A** under the conditions of run 3, which was used as the standard for the synthesis of the star polymer in subsequent experiments. Incidentally, the formation of linear polymers directly initiated with the $[Rh(nbd)Cl]_2$ is negligible under these conditions because the MALDI-FT-ICR-MS spectra of the oligomers synthesized under the same conditions with a different feed ratio ([**1**]/([**A**]/3) = 10) exhibited peaks attributable only to star polymers (Fig. S1†).[20]

Next, block-type star polymers were synthesized by exploiting the features of living polymerization using this catalyst system. After the first monomer **1** was completely consumed, an equal amount of a second monomer **2** was added to the polymerization solution, and the polymerization reaction continued. This yielded block-type star polymers with a narrow molecular weight dispersion (Scheme 2 and Fig. 2). The composition of the two monomers (**1** and **2**) in the copolymer was estimated to be [**1**] : [**2**] = 1 : 1 based on the analysis of their ^{1}H NMR spectra (Fig. S2† and Table 2). Notably, the polymerization time of the first feed monomer significantly affected the molecular weight distribution of the resulting copolymers. When the polymerization time of the first feed monomer was longer than 1 h, the intensity of the shoulder peak in the low-molecular-weight region increased with time in the SEC measurement of the resulting copolymers (Fig. S3†). This may be because the Rh complex at the growing chain end is gradually deactivated, probably owing to an undesired termination reaction. However, when the second monomer was added immediately after the first feed monomer was consumed (20 min), star-shaped block copolymers with narrow molecular weight dispersions were obtained (Fig. 2).

To confirm whether initiator **A** functioned as a trifunctional initiator, hydrolyzable initiator **B** was designed and synthesized by introducing a phenylpinacol borate group *via* an ester group (Scheme S2†) so that the arm polymer chain could be isolated from the star polymer core by hydrolysis after polymerization. Similar to the case using initiator **A**, the star polymers were synthesized by the polymerization of phenylacetylene (**1**) with a multicomponent catalyst system using initiator **B**. Consequently, the corresponding star polymer (**B**(poly-$\mathbf{1}_{50}$)$_3$) with a narrow molecular weight dispersion was obtained in high yield (Scheme 3). Treatment of the obtained star polymer **B**(poly-$\mathbf{1}_{50}$)$_3$ with 40% tetra-*n*-butylammonium hydroxide (TBAOH) for 2 h resulted in the quantitative cleavage of the arm polymer chains from the core by hydrolysis of the ester group (Schemes 3 and S8†). As shown in Fig. 3, SEC measurements

Table 2 Results of multistage copolymerization of phenylacetylenes (1st stage: **1**, 2nd stage: **2**) with a Rh-based multicomponent catalyst system using initiator A[a]

			Polymer			
run	[**1**]/([**A**]/3)	[**2**]/([**A**]/3)	Sample code	Yield[b] (%)	$M_n \times 10^{-4}$[c]	M_w/M_n[c]
4	50	50	**A**(poly($\mathbf{1}_{50}$-*b*-$\mathbf{2}_{50}$))$_3$	94	2.9	1.05
5	250	250	**A**(poly($\mathbf{1}_{250}$-*b*-$\mathbf{2}_{250}$))$_3$	85	9.3	1.35

[a] Reaction conditions: **A** (0.10 mmol), $[Rh(nbd)Cl]_2$ (0.067 mmol), DPA (0.2 mmol), in THF (0.2 mL) at 0 °C for 10 min, then phenylacetylene (**1**) (1.7 mmol (run 4), 8.5 mmol (run 5)) and PPh_3 (0.2 mmol) in THF (3.8 mL) at 30 °C for 20 min. Then, monomer (**2**) (1.7 mmol (run 4), 8.5 mmol (run 5)) was added. [b] Methanol-insoluble part. [c] Determined by SEC using three columns (TSKgel G4000H$_{XL}$ + G3000H$_{XL}$ + G3000H$_{XL}$) connected in series (run 4) or one column (KF-805L) (run 5) based on polystyrene standards (THF, 40 °C).

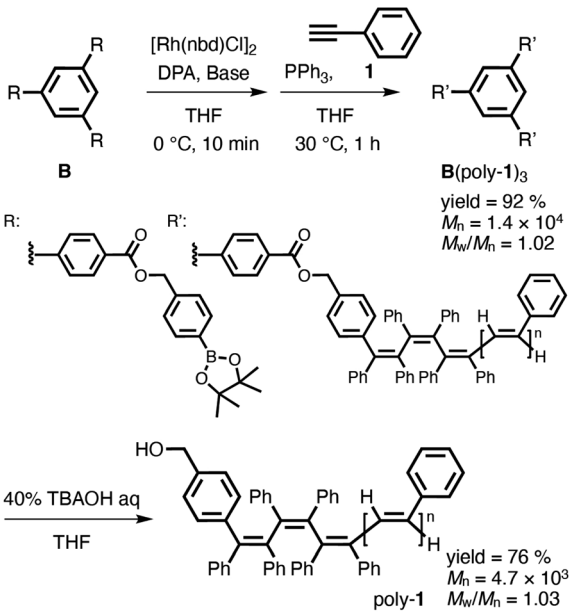

Scheme 3 Synthesis of star polymer B(poly-$\mathbf{1}$)$_3$ using hydrolyzable initiator B and isolation of the arm polymers (poly-$\mathbf{1}$) by its hydrolysis.

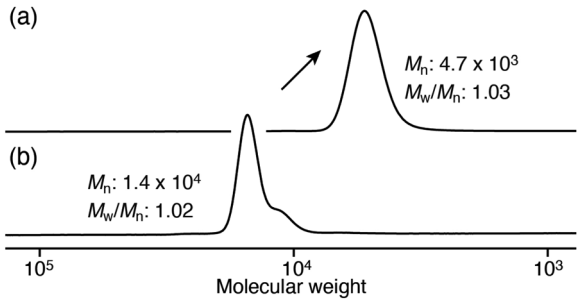

Fig. 3 SEC chromatograms of star polymer B(poly-$\mathbf{1}_{50}$)$_3$ (a) and the isolated arm polymer (poly-$\mathbf{1}$) by hydrolysis of B(poly-$\mathbf{1}_{50}$)$_3$ (b).

revealed that the resulting isolated arm polymer had a very narrow molecular weight dispersion (M_w/M_n = 1.03), and its molecular weight was almost the same as that expected from the feed ratio (M_n = 4.7 × 10^3). These results clearly demonstrate that initiators **A** and **B** efficiently functioned as trifunctional initiators in the polymerization of phenylacetylene (**1**) with a multicomponent catalyst system.

AFM observation and the chiroptical properties of optically active poly(phenylacetylene)s bearing alanine-derived pendants have been reported by Yashima and coworkers.[29–31] To directly observe the star polymers by AFM and investigate the effect of star polymer topology on their thermal properties and chiral amplification properties, two types of optically active star polymers with a different arm length (25- and 500-mers) (**A**(poly-$\mathbf{3}R_{25}$ or $\mathbf{3}S_{25}$)$_3$ and **A**(poly-$\mathbf{3}R_{500}$ or $\mathbf{3}S_{500}$)$_3$) were synthesized by the polymerization of $\mathbf{3}R$ and $\mathbf{3}S$ with the multicomponent catalyst system using initiator **A** (Scheme 4 and Table 3). Optically active star polymers (**A**(poly-$\mathbf{3}R_{25}$)$_3$ and **A**(poly-$\mathbf{3}S_{25}$)$_3$) with small M_w/M_n values (1.02 and 1.03, respectively) were quantitatively

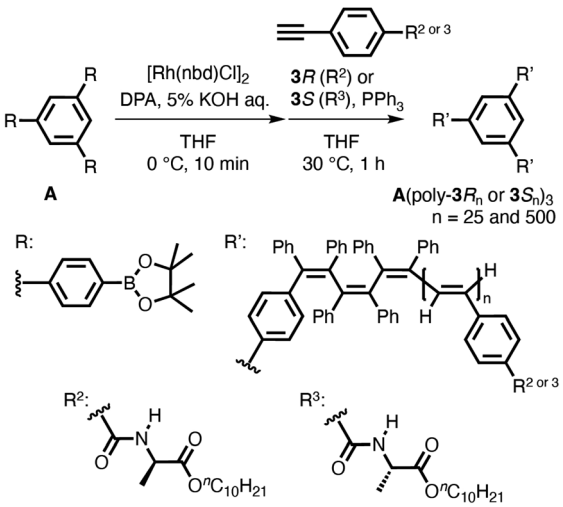

Scheme 4 Synthesis of optically active star polymers (A(poly-$\mathbf{3}R_n$)$_3$ and A(poly-$\mathbf{3}S_n$)$_3$, n = 25 and 500) using initiator A.

obtained when the feed ratio ([$\mathbf{3}S$ or $\mathbf{3}R$]/([**A**]/3)) was 25 (runs 6 and 7 in Table 3 and Fig. 4a, b). In contrast, the M_w/M_n values of the high-molecular-weight star polymers (**A**(poly-$\mathbf{3}R_{500}$)$_3$ and **A**(poly-$\mathbf{3}S_{500}$)$_3$), which were synthesized at a feed ratio ([$\mathbf{3}S$ or $\mathbf{3}R$]/([**A**]/3)) of 500 (runs 8 and 9 in Table 3 and Fig. 4c, d), increased (to 1.48 and 1.60, respectively).[20]

The topology of the optically active star polymer with a high molecular weight (**A**(poly-$\mathbf{3}R_{500}$)$_3$) was directly observed using AFM. Fig. 5 shows a typical amplitude-modulation AFM (AM-AFM) height image of **A**(poly-$\mathbf{3}R_{500}$)$_3$ on a mica substrate. The AFM image shows that many **A**(poly-$\mathbf{3}R_{500}$)$_3$ molecules have a three-armed star structure. A high-magnification AFM image of a single **A**(poly-$\mathbf{3}R_{500}$)$_3$ molecule is shown in Fig. 5b. Individual arms of the star-shaped polymer with an average height of approximately 1.6 nm are clearly observed (Fig. 5c), and the exact length of each arm of the star-shaped polymer was determined. Fig. 5d shows the length distribution of the arms of **A**(poly-$\mathbf{3}R_{500}$)$_3$ obtained by analyzing the AFM images of more than 45 isolated star polymers (Fig. S4†); the average length of the individual arms of **A**(poly-$\mathbf{3}R_{500}$)$_3$ was 84.5 nm, which is slightly shorter than the estimated length. However, the length of each arm within an individual **A**(poly-$\mathbf{3}R_{500}$)$_3$ molecule was roughly uniform (75–85 nm), confirming that polymerization was precisely controlled. The absolute weight-average molecular weight (M_w) of **A**(poly-$\mathbf{3}R_{500}$)$_3$ was determined to be 4.30 × 10^5 using SEC-MALS. From this result, the average arm length of **A**(poly-$\mathbf{3}R_{500}$)$_3$ was calculated to be 83 nm, which is consistent with the average length estimated from the AFM analysis. The AFM images of **A**(poly-$\mathbf{3}R_{500}$)$_3$ (Fig. 5a and S4†) show that most polymer molecules have three arms, although a small number of two-armed and linear polymers was also observed. Therefore, the AFM observation also directly corroborates that, in this polymerization system, almost all initiating sites of the initiator core initiated the polymerization reaction, and the polymerization reaction does not stop halfway and yields an uniform molecular length.

Table 3 Polymerization results of chiral phenylacetylenes (3*R* and 3*S*) with a Rh-based multicomponent catalyst system using initiator **A**[a]

Run	Monomer	[3]/([**A**]/3)	Polymer			
			Sample code	Yield[b] (%)	$M_n \times 10^{-4}$[c]	M_w/M_n[c]
6	3*R*	25	**A**(poly-3R_{25})$_3$	95	2.0	1.02
7	3*S*	25	**A**(poly-3S_{25})$_3$	90	2.1	1.03
8	3*R*	500	**A**(poly-3R_{500})$_3$	83	33.4	1.48
9	3*S*	500	**A**(poly-3S_{500})$_3$	80	32.7	1.60

[a] Reaction conditions: **A** (0.10 mmol), $[Rh(nbd)Cl]_2$ (0.067 mmol), DPA (0.2 mmol), in THF (0.2 mL) at 0 °C for 10 min, then phenylacetylene (**1**) (0.85 mmol (runs 6 and 7), 17.0 mmol (runs 8 and 9)) and PPh_3 (0.2 mmol) in THF (3.8 mL) at 30 °C for 1 h. [b] Methanol-insoluble part. [c] Determined by SEC using three columns (TSKgel G4000H_{XL} + G3000H_{XL} + G3000H_{XL}) connected in series (runs 6 and 7) or one column (KF-805L) (runs 8 and 9) based on polystyrene standards (THF, 40 °C).

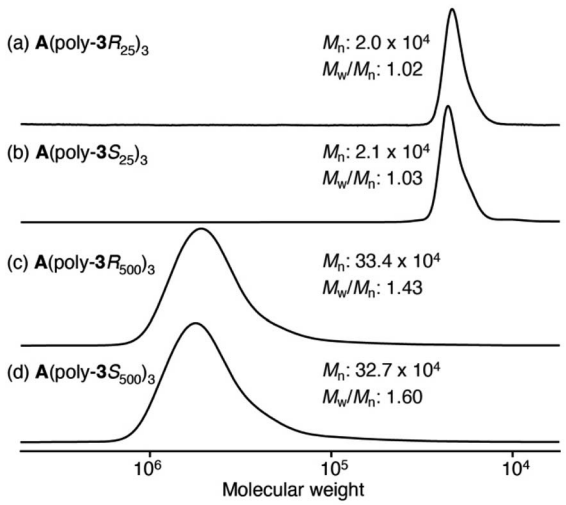

Fig. 4 SEC chromatograms of chiral star polymers (a) and (c) **A**(poly-3R_n)$_3$ and (b) and (d) **A**(poly-3S_n)$_3$ (n = 25 and 500).

To investigate the effect of polymer topology on thermal properties and chiral amplification in helical poly(phenylacetylene) chains, the chiral properties of star polymers **A**(poly-3S_{25})$_3$ and **A**(poly-3R_{25})$_3$ were compared with those of the corresponding linear polymers of the same length (poly-3S_{25} and poly-3R_{25}, respectively), which were synthesized by the polymerization of 3*S* and 3*R* with a multicomponent catalyst system using 4-methylphenylboronic acid as the initiator (Scheme S7†). For the star polymers, since one chain end of the arm polymer is anchored to the central core, which could influence the conformational rigidity, the thermal transition of the main chain was investigated using DSC. An exothermic peak was observed at approximately 170 °C in both the chiral star polymer and the linear polymer with the same chain length (25 mer) (Fig. S5†), suggesting a possible *cis–trans* transition.[27] This result suggests that the star polymer topology does not significantly influence the thermal transition of the main chain. The absorption and circular dichroism (CD) spectra of the polymers in THF and toluene are shown in Fig. 6a and b, respectively. In THF, the star polymers exhibited larger CD intensities than the corresponding linear polymers (Fig. 6a). In contrast, in toluene, the CD intensities of the star and linear polymers are almost the same (Fig. 6b). Thus, chiral amplification derived from the unique structure of the star polymer was confirmed for THF. The chiral amplification observed for

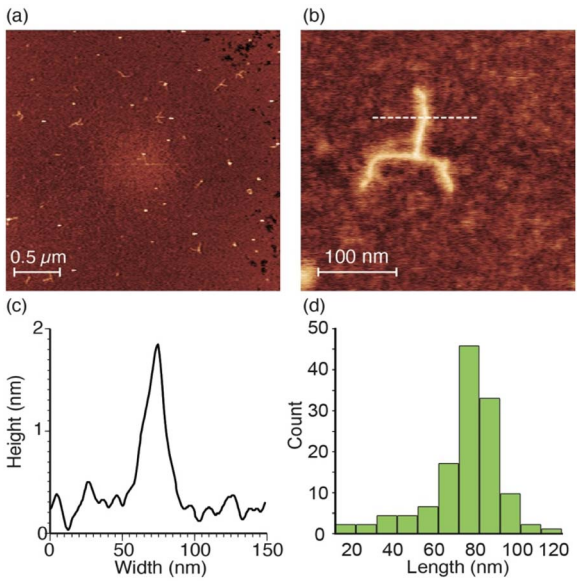

Fig. 5 AFM images of star polymer **A**(poly-3R_{500})$_3$. (a) Topographic image of **A**(poly-3R_{500})$_3$ prepared by spin casting a dilute toluene solution onto mica. (b) Magnified image of **A**(poly-3R_{500})$_3$ on mica. (c) Line profile along the white dashed line in (b). (d) Histogram showing the length distribution of the arm polymers of the star polymers obtained from several AFM images.

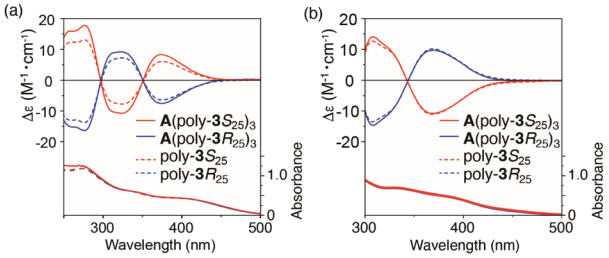

Fig. 6 CD and absorption spectra of optically active star polymers (**A**(poly-3S_{25})$_3$ and **A**(poly-3R_{25})$_3$) and the corresponding linear polymers (poly-3S_{25} and poly-3R_{25}) in THF at −10 °C (a) and in toluene at −10 °C (b).

the star polymers could be largely attributed to the effect of change in the flexibility at the polymer chain ends. In star polymers, one end of the polymer chain is anchored to the central core; therefore, the effect of the flexible polymer chain ends is reduced compared with that of the corresponding linear polymer. Therefore, in THF, where intramolecular hydrogen bonding between the side-chain amide groups is prevented,[32] chiral amplification was observed in the star polymer, which is less affected by this flexible chain end, compared to the linear polymer. In contrast, in toluene, the helical structures of both polymers are strongly stabilized by the intramolecular hydrogen bonds between the pendant amide groups;[32] therefore, it was assumed that the effect of the polymer ends was hardly observed.

Conclusions

In summary, we have synthesized three-armed star-shaped poly(phenylacetylene) chains by the Rh-catalyzed living polymerization of phenylacetylenes using trifunctional initiators and investigated their structures and chiral amplification properties. SEC analysis of the arms detached from the star polymers by hydrolysis clearly demonstrated that polymerization was uniformly initiated from almost all the boric acid groups present in the trifunctional initiators, resulting in star polymers with a precisely controlled arm length. Direct visualization of the polymers by AFM also clearly corroborated the formation of star polymers with a precisely controlled structure. Furthermore, optically active star polymers synthesized from chiral monomers were, for the first time, confirmed to exhibit chiral amplification because of their unique topological structures. These findings will be useful for designing and synthesizing topologically unique star polymers consisting of dynamic helical polymers to develop functional chiral materials that can be applied in materials science and nanotechnology.

Author contributions

TN and TT conceived of the study. AI and MY synthesized the star polymers and conducted several analyses. SD, AY, KM and TF contributed to the AFM measurements. SK and MK contributed to the MALS SEC measurements. TN and KM drafted the manuscript and supervised the study. All the authors reviewed the draft manuscript and critically revised it for intellectual content. All authors have approved the final version of the manuscript for publication.

Conflicts of interest

There are no conflicts to declare.

Acknowledgements

This work was partially supported by JSPS KAKENHI (Grant-in-Aid for Specially Promoted Research, No. JP18H05209 (K. M.) and Grant-in-Aid for Scientific Research (A), No. JP21H04691 (K. M.) and Grant-in-Aid for Fostering Joint International Research (B), No. JP21KK0084 (T. N.) and Grant-in-Aid for Scientific Research (C), No. JP21K04685 (T. N.) and JP19K06972 (T. T.)), and the World Premier International Research Center Initiative (WPI), MEXT, Japan.

Notes and references

1 J. M. Ren, T. G. McKenzie, Q. Fu, E. H. H. Wong, J. Xu, Z. An, S. Shanmugam, T. P. Davis, C. Boyer and G. G. Qiao, *Chem. Rev.*, 2016, **116**, 6743–6836.
2 B. Mendrek, N. Oleszko-Torbus, P. Teper and A. Kowalczuk, *Prog. Polym. Sci.*, 2023, **139**, 101657.
3 L. Y. Qiu and Y. H. Bae, *Pharm. Res.*, 2006, **23**, 1–30.
4 D.-P. Yang, M. N. N. L. Oo, G. R. Deen, Z. Li and X. J. Loh, *Macromol. Rapid Commun.*, 2017, **38**, 1700410.
5 K. Aoi, H. Suzuki and M. Okada, *Macromolecules*, 1992, **25**, 7073–7075.
6 Y. Miura, *Polym. J.*, 2012, **44**, 679–689.
7 T. Fujiyabu, Y. Yoshikawa, U.-i. Chung and T. Sakai, *Sci. Technol. Adv. Mat.*, 2019, **20**, 608–621.
8 L. Cosimbescu, J. W. Robinson, Y. Zhou and J. Qu, *RSC Adv.*, 2016, **6**, 86259–86268.
9 M. Ouchi and M. Sawamoto, *Macromolecules*, 2017, **50**, 2603–2614.
10 K. Matyjaszewski, *Macromolecules*, 2012, **45**, 4015–4039.
11 M. Semsarilar and S. Perrier, *Nat. Chem.*, 2010, **2**, 811–820.
12 H. Gao and K. Matyjaszewski, *Prog. Polym. Sci.*, 2009, **34**, 317–350.
13 D. A. Siriwardane, O. Kulikov, J. F. Reuther and B. M. Novak, *Macromolecules*, 2017, **50**, 832.
14 N. Liu, L. Zhou and Z.-Q. Wu, *Acc. Chem. Res.*, 2021, **54**, 3953–3967.
15 T. Miyabe, H. Iida, M. Banno, T. Yamaguchi and E. Yashima, *Macromolecules*, 2011, **44**, 8687–8692.
16 H. Hasegawa, Y. Nagata, K. Terao and M. Suginome, *Macromolecules*, 2017, **50**, 7491–7497.
17 Y.-X. Xue, Y.-Y. Zhu, L.-M. Gao, X.-Y. He, N. Liu, W.-Y. Zhang, J. Yin, Y. Ding, H. Zhou and Z.-Q. Wu, *J. Am. Chem. Soc.*, 2014, **136**, 4706–4713.
18 Y. Wang, A. L. Kanibolotsky, P. J. Skabara and T. Nakano, *Chem. Commun.*, 2016, **52**, 1919–1922.
19 N. Kanbayashi, K. Yamazaki, M. Nishio and K. Onitsuka, *Macromolecules*, 2022, **55**, 5027–5037.
20 T. Taniguchi, T. Yoshida, K. Echizen, K. Takayama, T. Nishimura and K. Maeda, *Angew. Chem., Int. Ed.*, 2020, **59**, 8670–8680.
21 S. Sakamoto, T. Taniguchi, Y. Sakata, S. Akine, T. Nishimura and K. Maeda, *Angew. Chem., Int. Ed.*, 2021, **60**, 22201–22206.
22 K. Echizen, T. Taniguchi, T. Nishimura and K. Maeda, *Angew. Chem., Int. Ed.*, 2022, **61**, e202202676.
23 K. Echizen, T. Taniguchi, T. Nishimura and K. Maeda, *J. Am. Chem. Soc.*, 2021, **143**, 3604–3612.
24 K. Kanki and T. Masuda, *Macromolecules*, 2003, **36**, 1500–1504.
25 E. Yashima, N. Ousaka, D. Taura, K. Shimomura, T. Ikai and K. Maeda, *Chem. Rev.*, 2016, **116**, 13752–13990.

26 F. Freire, E. Quiñoá and R. Riguera, *Chem. Rev.*, 2016, **116**, 1242–1271.
27 S. Wang, X. Feng, J. Zhang, P. Yu, Z. Guo, Z. Li and X. Wan, *Macromolecules*, 2017, **50**, 3489–3499.
28 Q. Wang, C. Yu, H. Long, Y. Du, Y. Jin and W. Zhang, *Angew. Chem., Int. Ed.*, 2015, **54**, 7550–7554.
29 S.-I. Sakurai, K. Okoshi, J. Kumaki and E. Yashima, *Angew. Chem., Int. Ed.*, 2006, **45**, 1245–1248.
30 S.-I. Sakurai, K. Okoshi, J. Kumaki and E. Yashima, *J. Am. Chem. Soc.*, 2006, **128**, 5650–5651.
31 S. Ohsawa, S.-I. Sakurai, K. Nagai, M. Banno, K. Maeda, J. Kumaki and E. Yashima, *J. Am. Chem. Soc.*, 2011, **133**, 108–114.
32 K. Okoshi, S.-I. Sakurai, S. Ohsawa, J. Kuniaki and E. Yashima, *Angew. Chem., Int. Ed.*, 2006, **45**, 8173–8176.